

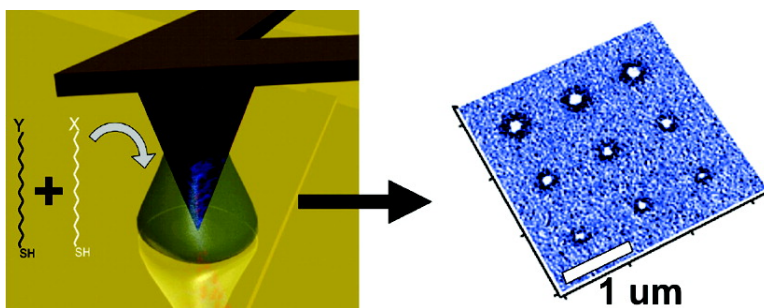
Article

Spontaneous “Phase Separation” of Patterned Binary Alkanethiol Mixtures

Khalid Salaita, Anand Amarnath, Daniel Maspoeh, Thomas B. Higgins, and Chad A. Mirkin

J. Am. Chem. Soc., **2005**, 127 (32), 11283-11287 • DOI: 10.1021/ja042393y • Publication Date (Web): 22 July 2005

Downloaded from <http://pubs.acs.org> on March 25, 2009



More About This Article

Additional resources and features associated with this article are available within the HTML version:

- Supporting Information
- Links to the 11 articles that cite this article, as of the time of this article download
- Access to high resolution figures
- Links to articles and content related to this article
- Copyright permission to reproduce figures and/or text from this article

[View the Full Text HTML](#)

Spontaneous “Phase Separation” of Patterned Binary Alkanethiol Mixtures

Khalid Salaita,[†] Anand Amarnath,[‡] Daniel Maspoch,[†] Thomas B. Higgins,[‡] and Chad A. Mirkin^{*†}

Contribution from the Department of Chemistry and Institute for Nanotechnology, Northwestern University, Evanston, Illinois 60208, and Harold Washington College, Chicago, Illinois 60601

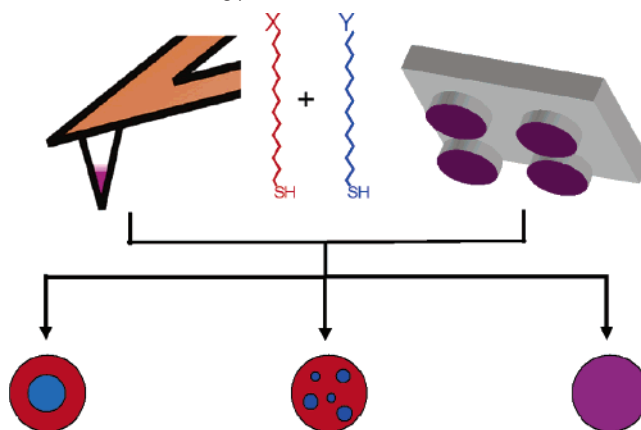
Received December 17, 2004; E-mail: camirkin@chem.northwestern.edu

Abstract: This article describes novel phase-separation behavior by a binary mixture of alkanethiols when deposited onto a gold surface using micro- and nanodeposition tools, such as microcontact printing (μ CP) and dip-pen nanolithography (DPN). This behavior is significantly different than that observed in the bulk. We demonstrate this behavior using three model compounds: 16-mercaptohexadecanoic acid (MHA), 1-octadecanethiol (ODT), and $\text{CF}_3(\text{CF}_2)_{11}(\text{CH}_2)_2\text{SH}$ (PFT). The identity of the resulting segregated structure is confirmed by lateral force microscopy (LFM) and by selective metal–organic coordination chemistry. Importantly, this phenomenon can be exploited to print sub-100 nm wide alkanethiol lines via conventional μ CP and to form sub-15 nm features using DPN, which is below the ultimate resolution of both these techniques. We also demonstrate that these nanopatterned materials can serve as templates for constructing more complex architectures.

Introduction

An understanding of the factors that control SAM formation and behavior both on the macro- and nanoscopic length scales is essential for scientists to reap their full potential. With the advent of molecular deposition tools, such as dip-pen nanolithography (DPN), it is now possible to study such processes on the nanometer to micrometer length scale.^{1–4} A fundamental issue with such deposition processes pertains to the transport properties of a binary mixture of ink molecules (Scheme 1). In particular, would the transport of such mixtures result in a nano- or microstructure with a homogeneous distribution of adsorbate molecules (far right), a structure with islandlike phase separation (middle), or a near-complete phase separation of the two adsorbates (far left)? The study of nanometer-scale mixing of binary monolayers is important for two reasons. First, it potentially allows one to elucidate the fundamental properties and origins of phase segregation for two-component mixtures on surfaces. Second, once understood, it could allow one to deliberately tailor desired surface properties at the sub-50 nm length scale. Herein, we report the results of patterning binary alkanethiol mixtures with hydrophobic and hydrophilic ω -functionalized tail groups. Interestingly, we have identified an unusual near-complete phase-separation process that results in nanostructures consisting of hydrophilic interiors and hydrophobic peripheries. This phenomenon extends beyond DPN to

Scheme 1. Possible Outcomes of Patterning a Binary Mixture of Two Alkanethiols Using μ CP and DPN



the lower resolution and high-throughput microcontact printing (μ CP)^{5–7} process and can be used to increase the resolution of both techniques under certain conditions.

Surprisingly few examples of nanometer-scale phase separation have been reported for binary SAM mixtures.^{8–12} Spon-

[†] Northwestern University.

[‡] Harold Washington College.

(1) Piner, R. D.; Zhu, J.; Xu, F.; Hong, S. H.; Mirkin, C. A. *Science* **1999**, *283*, 661–663.

(2) Ginger, D. S.; Zhang, H.; Mirkin, C. A. *Angew. Chem., Int. Ed.* **2004**, *43*, 30–45.

(3) Hong, S. H.; Zhu, J.; Mirkin, C. A. *Science* **1999**, *286*, 523–525.

(4) Hong, S. H.; Zhu, J.; Mirkin, C. A. *Langmuir* **1999**, *15*, 7897–7900.

(5) Kumar, A.; Whitesides, G. M. *Science* **1994**, *263*, 60–62.

(6) Odom, T. W.; Love, J. C.; Wolfe, D. B.; Paul, K. E.; Whitesides, G. M. *Langmuir* **2002**, *18*, 5314–5320.

(7) Gates, B. D.; Xu, Q. B.; Love, J. C.; Wolfe, D. B.; Whitesides, G. M. *Annu. Rev. Mater. Res.* **2004**, *34*, 339–372.

(8) Stranick, S. J.; Parikh, A. N.; Tao, Y. T.; Allara, D. L.; Weiss, P. S. *J. Phys. Chem.* **1994**, *98*, 7636–7646.

(9) Imabayashi, S.; Hobara, D.; Kakiuchi, T.; Knoll, W. *Langmuir* **1997**, *13*, 4502–4504.

(10) Tamada, K.; Hara, M.; Sasabe, H.; Knoll, W. *Langmuir* **1997**, *13*, 1558–1566.

(11) Hayes, W. A.; Kim, H.; Yue, X. H.; Perry, S. S.; Shannon, C. *Langmuir* **1997**, *13*, 2511–2518.

(12) Jackson, A. M.; Myerson, J. W.; Stellacci, F. *Nat. Mater.* **2004**, *3*, 330–336.

taneous but random phase separation has been observed in scanning tunneling microscope (STM) images of coadsorbed alkanethiol mixtures on atomically flat gold surfaces.^{8,9,12–14} It has been established that the phase separation of mixed SAMs is a process driven by polar headgroup interactions and cohesive interactions between the adsorbate molecules. In such systems, the adsorbates randomly form nanoscale domains with no particular order.¹⁴ Phase-separated binary SAMs have been shown to be useful in resisting nonspecific protein adsorption,¹² improving DNA hybridization,¹⁵ improving the data quality in microarrays,¹⁶ and facilitating adsorption of cytochrome C.¹⁷ Note that the use of the term “phase separation” in the context of monolayer structures is not meant to imply the realization of an equilibrated system, but rather a concentration of each of the two adsorbates in assignable areas on the substrate.

Experimental Section

Materials. Polycrystalline Au films were prepared by evaporating 10 nm of Ti on SiO₂, followed by 60 nm of Au at room temperature.^{18,19} 16-Mercaptohexadecanoic acid (MHA) (90%), 1-octadecanethiol (ODT) (98%), fullerene (C₆₀) (99.9%), and copper(II) perchlorate hexahydrate (98%) were purchased from Aldrich Chemical Co., Milwaukee, WI. Acetonitrile (reagent grade) and toluene (99.9%) were purchased from Fisher Scientific. Ethanol (ACS/USP grade) was purchased from Pharmco Products, Inc., Brookfield, CT. All chemicals were used as received. 1*H*,1*H*,2*H*,2*H*-perfluorododecylthiol CF₃(CF₂)₁₁(CH₂)₂SH (PFT) was synthesized and purified according to literature procedures.^{20,21} Briefly, CF₃(CF₂)₁₁(CH₂)₂I (1-iodo-1*H*,1*H*,2*H*,2*H*-perfluorododecane, 97%, SynQuest Labs, Alachua, FL, www.synquestlabs.com) was converted to the thioacetate derivative using excess potassium thioacetate under refluxing methanol. The product was deprotected to the thiol derivative under a refluxing 3 M NaOH solution in acetone.²²

Dip-Pen Nanolithography, Micro Contact Printing, and Imaging. DPN experiments were performed with an atomic force microscope (AFM, CP, Veeco/Thermomicroscopes, Sunnyvale, CA) equipped with a 100 μm scanner and closed-loop scan control and commercial lithography software (DPNWrite, DPN System-1, NanoInk, Inc., Chicago, IL). Gold-coated commercial AFM cantilevers (sharpened Si₃N₄, Type A, NanoInk, Inc.) with a spring constant of 0.05 N/m were used for patterning and subsequent imaging. All DPN patterning experiments were carried out under ambient laboratory conditions (~30% relative humidity, ~20 °C), unless stated otherwise. Controlled atmosphere experiments were conducted inside a N₂ atmosphere glovebox, where organic solvents could be introduced. Tapping mode images were taken with a Nanoman AFM equipped with a Nanoscope IV controller from Veeco (Santa Barbara, CA) with silicon tips (NCH-W, Veeco, spring constant 40 N/m) scanned at a rate of 0.5 Hz and set to a pixel resolution of 512 × 512. Binary-inking solutions were prepared as a 1:1 mixture of two alkanethiols in ethanol, where the total alkanethiol concentration was 1 mM. Tips were soaked in this

solution for a few seconds and subsequently dried under a stream of N₂. This was generally repeated three times before the tip was used for patterning. Pure MHA-coated tips were prepared by immersing the cantilevers in an acetonitrile solution saturated with MHA for a few seconds, followed by blowing dry under a stream of nitrogen. Pure ODT-coated tips were prepared by thermal evaporation of neat ODT onto the tips at 65 °C for 30 min.

Micropatterns were generated via μCP. Stamps were fabricated by placing a photolithographically prepared master (photomask supplied by ADTEK, Quebec, Canada) in a glass Petri dish, followed by pouring a mixture of polydimethylsiloxane (PDMS, Sylgard 184, Dow Corning, Midland, MI) in the ratio of 10:1 (v:v) monomer to initiator over the master. After letting the mixture sit for 1 h to degas, the elastomer was cured overnight at 60 °C and then gently peeled from the master. The stamp was “inked” with a 1 mM total alkanethiol binary ink solution by gently spreading a drop on the surface of the stamp using a cotton swab. After the stamp was dry, patterned structures were generated on the surface by bringing the stamp (by hand) into contact with a clean Au substrate for 30 s.

Results and Discussion

In our experiments, we studied three different alkanethiol inks to investigate the formation of phase-separated structures in the context of DPN and μCP experiments: MHA, ODT, and PFT. These compounds were selected to take advantage of different driving forces for phase separation. MHA and ODT are almost identical in molecular weight and structure with the exception of the ω-terminal group, where the acid groups of MHA can participate in hydrogen bonding. On the other hand, PFT is a shorter hydrophobic molecule that will have significantly weaker adhesive interactions with MHA.

To explore the directed nanoscale behavior of these alkanethiol ink mixtures, AFM cantilevers were coated in binary ink mixtures and subsequently used for patterning. As an initial experiment, an MHA and ODT binary mixture coated AFM tip was held in contact with a gold surface for 8, 4, and 2 s three times, and the contact area was subsequently imaged using the same tip by lateral force microscopy (LFM) (Figure 1A). A central white (high contrast, high lateral force) domain can be seen that represents an area predominantly coated with MHA, while an outer dark ring (low contrast, low lateral force) representing mostly ODT is seen at the perimeter of each of the dots.²³ When a binary mixture of MHA and PFT is simultaneously deposited, similar structures with slightly higher LFM contrast form (Figure 1B). Although dots consist of two molecules, the diameter of each phase still shows $t^{1/2}$ dependence in accordance with our ink transport model and the model put forth by Jang et al. and used thus far to describe the DPN process (Figure 1C).^{24–27} Interestingly, when an MHA/ODT tip is brought into contact with the surface repeatedly, ring-type structures are formed (Figure 1D), where each time the tip is held in contact with the surface an additional two rings are formed (one predominantly MHA, and the other is predominantly ODT; see Supporting Information).

- (13) Stranick, S. J.; Atre, S. V.; Parikh, A. N.; Wood, M. C.; Allara, D. L.; Winograd, N.; Weiss, P. S. *Nanotechnology* **1996**, *7*, 438–442.
- (14) Lewis, P. A.; Smith, R. K.; Kelly, K. F.; Bumm, L. A.; Reed, S. M.; Clegg, R. S.; Gunderson, J. D.; Hutchison, J. E.; Weiss, P. S. *J. Phys. Chem. B* **2001**, *105*, 10630–10636.
- (15) Satjapipat, M.; Sanedrin, R.; Zhou, F. M. *Langmuir* **2001**, *17*, 7637–7644.
- (16) Datwani, S. S.; Vijayendran, R. A.; Johnson, E.; Biondi, S. A. *Langmuir* **2004**, *20*, 4970–4976.
- (17) Hobara, D.; Imabayashi, S.; Kakiuchi, T. *Nano Lett.* **2002**, *2*, 1021–1025.
- (18) Weinberger, D. A.; Hong, S.; Mirkin, C. A.; Wessels, B. W.; Higgins, T. B. *Adv. Mater.* **2000**, *12*, 1600–1603.
- (19) Zhang, Y.; Salaita, K.; Lim, J. H.; Lee, K. B.; Mirkin, C. A. *Langmuir* **2004**, *20*, 962–968.
- (20) Bain, C. D.; Troughton, E. B.; Tao, Y. T.; Evall, J.; Whitesides, G. M.; Nuzzo, R. G. *J. Am. Chem. Soc.* **1989**, *111*, 321–335.
- (21) Chidsey, C. E. D.; Loiacono, D. N. *Langmuir* **1990**, *6*, 682–691.
- (22) Zheng, T. C.; Burkart, M.; Richardson, D. E. *Tetrahedron Lett.* **1999**, *40*, 603–606.

- (23) Ivanisevic, A.; McCumber, K. V.; Mirkin, C. A. *J. Am. Chem. Soc.* **2002**, *124*, 11997–12001.
- (24) Rozhok, S.; Piner, R.; Mirkin, C. A. *J. Phys. Chem. B* **2003**, *107*, 751–757.
- (25) Jang, J. Y.; Hong, S. H.; Schatz, G. C.; Ratner, M. A. *J. Chem. Phys.* **2001**, *115*, 2721–2729.
- (26) Rozhok, S.; Sun, P.; Piner, R.; Lieberman, M.; Mirkin, C. A. *J. Phys. Chem. B* **2004**, *108*, 7814–7819.
- (27) For alternative model see: Sheehan, P. E.; Whitman, L. J. *Phys. Rev. Lett.* **2002**, *88*, 156104–156107.

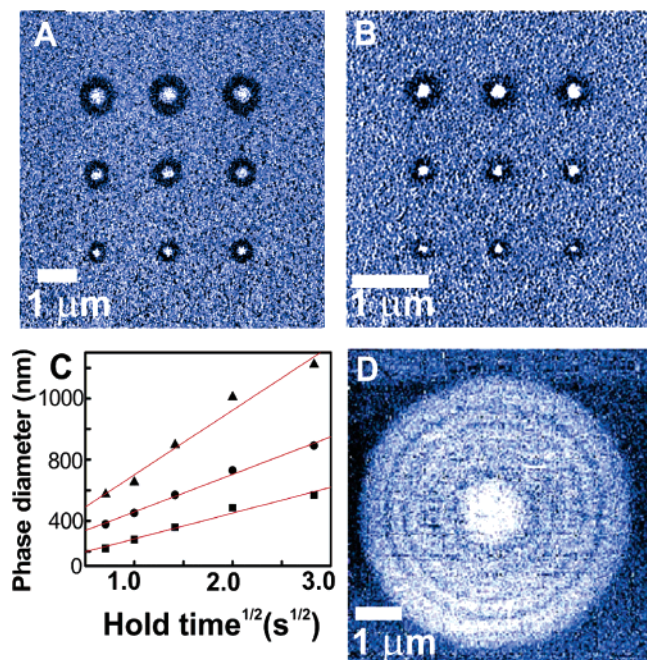


Figure 1. LFM images of phase-separated structures patterned on a Au surface with binary ink coated tip. (A) MHA interior and ODT exterior dots and (B) MHA interior and PFT exterior dots formed by holding the tip for 8, 4, and 2 s. (C) Plot of phase diameter versus holding time, showing $t^{1/2}$ dependence for MHA/ODT dots (triangles, circles, and square represent entire dot, ODT phase, and MHA phase, respectively). (D) MHA/ODT ring structure made by repeatedly approaching surface (five times).

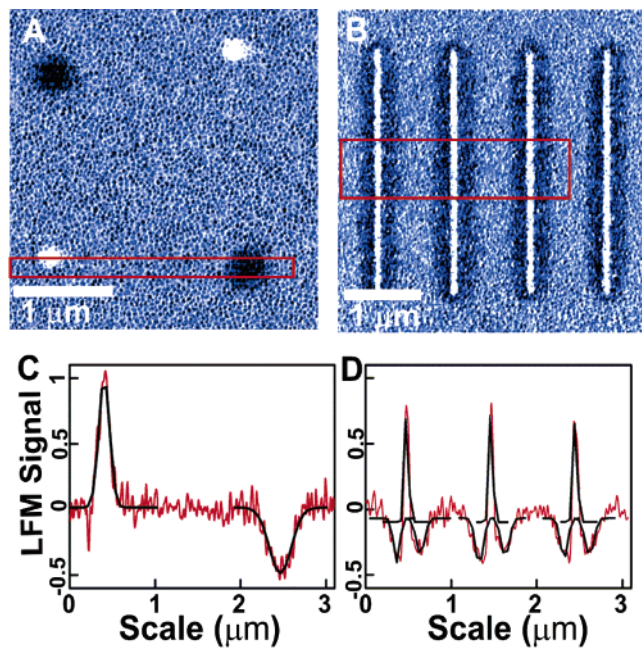


Figure 2. Comparison of the LFM properties of pure and phase-separated DPN-deposited alkanethiols on Au. (A) LFM image of pure MHA (white) and pure ODT (black) dots formed by DPN. (B) Four phase-separated MHA/PFT lines deposited by moving coated cantilever at a rate of $0.4 \mu\text{m/s}$. Corresponding plots show analyses of highlighted regions in each LFM image, where the black line represents a Gaussian fit of averaged line scans (red).

Phase-separation behavior is also independent of the path of the tip, and separated line structures assemble as an MHA/PFT tip is scanned in a line at a rate of $0.2 \mu\text{m/s}$ (Figure 2B), where the interior of the structure is composed of primarily MHA and the exterior of mostly PFT. To obtain a better understanding of

the degree of phase separation, we also patterned structures comprised of pure MHA and ODT (Figure 2A). The averaged frictional force profiles generated in these experiments show bands associated with patterns of MHA and ODT (Figure 2C). The frictional force profiles were modeled as Gaussian distributions, and the peaks of these plots were used to evaluate the distribution of the two components in patterned binary structures. The friction force profile of segregated structures (Figure 2D) shows less intense peaks ($\sim 80\%$) than those of pure adsorbates (Figure 2C). This indicates that near-complete segregation is observed in the experiment described in Figure 2B. The interior of these structures is always comprised of the more hydrophilic MHA, and this remains true even when patterning is performed in an inert atmosphere saturated with methanol (see Supporting Information).

Comparison of LFM images collected from pure and mixed-ink nanostructures suggests that mixtures of alkanethiols do indeed phase separate into domains. However, factors such as molecular packing and orientation can have a contribution to the observed frictional force signal.^{28,29} Many surface spectroscopic techniques, such as XPS or grazing angle FT-IR, are capable of discriminating between different alkanethiols, but this is not feasible for sub-100 nm features. In addition, the heights of alkanethiols used in this study are very similar, and subsequently, height mode images are not useful for discriminating between the two different molecules, especially on polycrystalline Au films with an RMS roughness of 1 nm. We, therefore, take advantage of the ability of the terminal acid groups of MHA to coordinate to metals, such as Cu^{2+} , and build metal–organic multilayers as demonstrated by Evans et al.³⁰ to provide additional evidence as to the chemical identity of the mixed-ink nanostructures. As described in Figure 1A, an MHA/ODT mixed-ink coated tip was used to pattern an array (3×3) of dots, and the resulting LFM image is shown in Figure 3A. The sample is then exposed to a 1 mM ODT solution in ethanol for 10 min, which renders unpatterned bare Au areas unreactive toward coordination to Cu^{2+} . Excess material is washed under a stream of ethanol and water, and the substrate is subsequently imaged in tapping mode. Patterned dots are undetectable in height mode (Figure 3B) since the heights of MHA and ODT are very similar. However, the interiors of these dots are detectable in phase mode (Figure 3C), which indicates that the interiors of these dots are different than the ODT-passivated exterior regions. A metal–organic coordinating layer is then selectively adsorbed onto the MHA areas by incubating the sample in a 1 mM CuClO_4 solution in ethanol for 15 min followed by rinsing and further immersing the Au film in a 1 mM MHA solution for 15 min. After removing physisorbed material with ethanol rinses, the sample is again imaged by using tapping mode to minimize sample damage. Height mode images (Figure 3D) show that only the interior regions of each of the dots have increased in height. Averaged line scan analyses of dots before (Figure 3E) and after (Figure 3F) coordination layer growth show that the interior region of each dot has increased in height by $1.6 \pm 0.1 \text{ nm}$. This value agrees with previously published results for the thickness of an MHA layer grown onto

(28) Overney, R. M.; Meyer, E.; Frommer, J.; Guntherodt, H. J.; Fujihira, M.; Takano, H.; Gotoh, Y. *Langmuir* **1994**, *10*, 1281–1286.

(29) Brewer, N. J.; Leggett, G. J. *Langmuir* **2004**, *20*, 4109–4115.

(30) Evans, S. D.; Ulman, A.; Goppertberarducci, K. E.; Gerenser, L. J. *J. Am. Chem. Soc.* **1991**, *113*, 5866–5868.

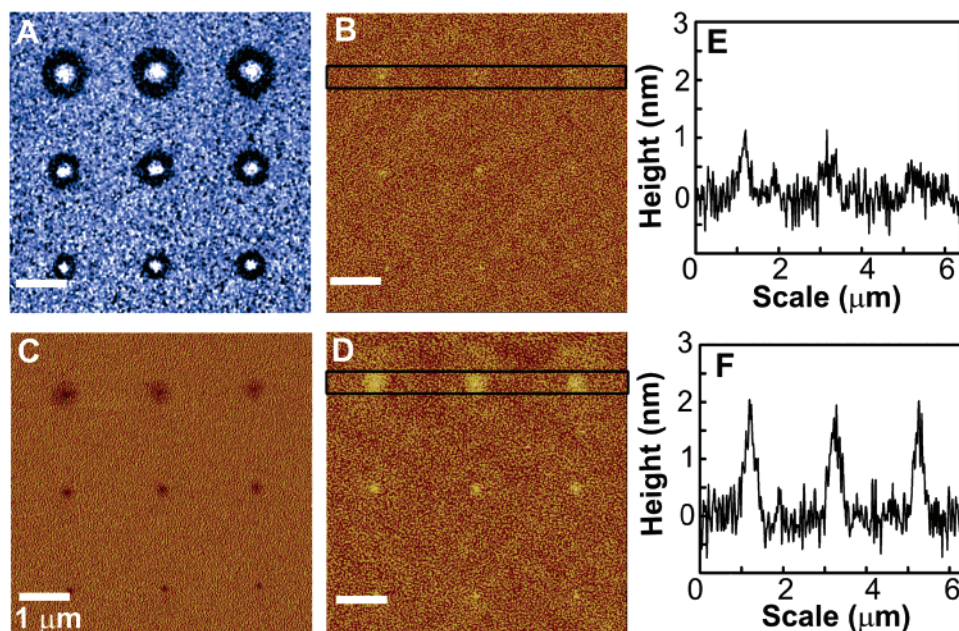


Figure 3. Probing the chemical composition of segregated binary ink patterns by utilizing selective metal–organic coordination to the terminal carboxy group of MHA. (A) LFM image of 3×3 MHA/ODT phase-separated dot array. (B) Tapping mode height and (C) corresponding phase image of an ODT-passivated dot array. Note that dots are of similar height to the background. (D) Tapping mode height image of dot array after coordinating a layer of MHA onto a Cu^{2+} -incubated substrate. Averaged line scans of mixed-ink dots (E) before and (F) after growth of the MHA layer, which show a height increase of 1.6 ± 0.1 nm only in the interior region of each dot.

a monolayer of Cu^+ .^{30,31} The chemical reactivity data agree with the frictional force data, thus showing that the more hydrophilic MHA will generate a central phase, while the more hydrophobic ODT will form an outer perimeter phase when the two alkanethiols are deposited simultaneously by DPN.

The observed phase separation in the patterned nanostructures is presumably the result of enthalpic contributions since entropy would favor mixing of the constituents within the generated patterns. Spontaneous phase separation driven by hydrogen bonding or van der Waals interactions is consistent with previous reports in bulk SAMs. Leggett et al. have determined that the contribution from hydrogen bonding within an acid-terminated monolayer is equivalent to the van der Waals stabilization of nine methylene groups.³² MHA is only two methylene groups shorter than ODT, and therefore, hydrogen bonding interactions would be expected to provide a major driving force for phase separation of a mixture of MHA and ODT. In the case of MHA/PFT mixtures, the driving force for phase separation is a combination of both hydrogen bonding as well as van der Waals interactions since there are only two methylene units in PFT. This may explain why LFM contrast in the MHA/ODT system is lower than that of MHA/PFT. The separation may also be enhanced by the water/air interface at the surface of the water meniscus formed during patterning.^{24,26,33} Furthermore, the kinetics of ink transport from tip to surface are certainly a factor in determining the ultimate nanopattern composition, especially with regard to adsorbate solubility and diffusion in water. For example, the solubility of MHA is at least 3 orders of magnitude larger than that of ODT.³⁴ As a result, MHA molecules will

certainly reach the Au surface at a more rapid rate than that of ODT. The difference of ink solubility in the meniscus explains why the predominantly MHA phase is always observed at the center of these binary structures. It also explains why introducing a methanol atmosphere influences the rate of transport and the magnitude of phase separation (see Supporting Information).

This phenomenon can, in principle, provide two advantages to a variety of chemical-based lithographies, such as μCP and DPN. First, it can potentially increase the ultimate resolution of a variety of these techniques, and second, it can simultaneously generate multicomponent structures. To demonstrate this, a binary mixture of 1:1 MHA:PFT ink (1 mM total concentration) was coated onto a poly(dimethylsiloxane) (PDMS) stamp, and the stamp was immediately applied onto a gold surface. The resulting patterns show phase-separated lines of alkanethiol (Figure 4A). The central region of the patterned lines is comprised of predominantly MHA, while the perimeter of these lines is made of predominantly PFT. Interestingly, the width of the PFT lines is 100 nm, which is 20 times smaller than the width of the stamp features ($2 \mu\text{m}$). These features are also 5 times smaller than what can typically be obtained using conventional μCP .⁶ Furthermore, only a few techniques are capable of patterning multicomponent structures at submicrometer resolution,^{3,35} and each suffers from drawbacks. Multicomponent patterning has been demonstrated using conventional μCP .^{36,37} However, multicomponent patterning has only been achieved at the micrometer length scale. Utilizing phase separation is advantageous because the pattern resolution and component registry are defined by the choice of ink pairs and by the stamp feature size. In addition, monolayer structures

(31) Hatzor, A.; Weiss, P. S. *Science* **2001**, *291*, 1019–1020.

(32) Cooper, E.; Leggett, G. J. *Langmuir* **1999**, *15*, 1024–1032.

(33) Jang, J. Y.; Schatz, G. C.; Ratner, M. A. *Phys. Rev. Lett.* **2004**, *92*.

(34) Solubility of ODT in water is 2.37×10^{-4} mg/L at 25 °C, while 8-hexadecanoic acid, $\text{C}_{16}\text{H}_{30}\text{O}_2$, which is closely related to MHA in chemical structure, has a solubility of 1.33×10^{-1} mg/L. (Meylan W. M.; Howard P. H. *Environ. Toxicol. Chem.* **1996**, *15*, 100).

(35) Gerding, J. D.; Willard, D. M.; Van Orden, A. *J. Am. Chem. Soc.* **2005**, *127*, 1106–1107.

(36) Tien, J.; Nelson, C. M.; Chen, C. S. *Proc. Natl. Acad. Sci. U.S.A.* **2002**, *99*, 1758–1762.

(37) Inerowicz, H. D.; Howell, S.; Regnier, F. E.; Reifengerger, R. *Langmuir* **2002**, *18*, 5263–5268.

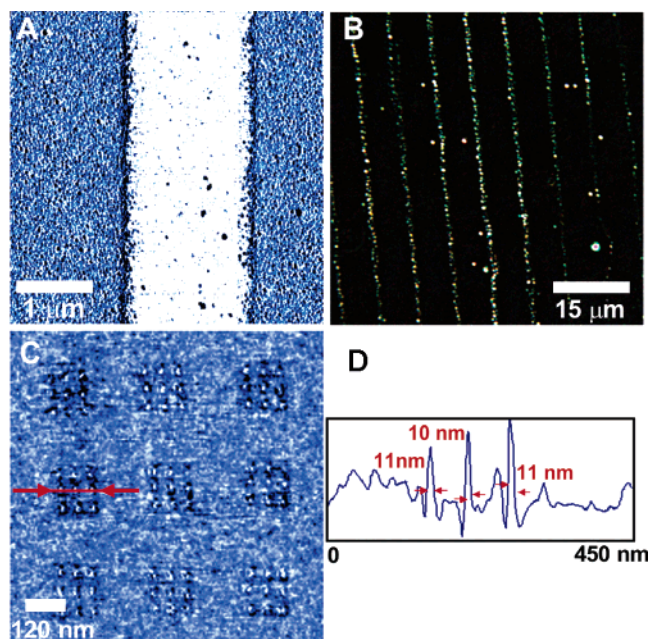


Figure 4. Exploiting phase separation of MHA/PFT to improve the resolution of DPN and μ CP. (A) LFM image of $2\ \mu\text{m}$ stamp applied onto a gold substrate. (B) Dark field micrograph of templated C_{60} aggregates onto (A) after passivation with MHA and incubation in $0.2\ \text{mg/mL}$ C_{60} solution in toluene. (C) DPN of binary mixed ink dots on a Au(111) surface, and (D) is the line scan profile through the highlighted region.

generated using the phase separation of binary ink mixtures can be further used to direct the assembly of a wide variety of materials. For example, when a 1:1 MHA:PFT stamped gold film (Figure 4A) is rendered hydrophilic by incubating in an MHA solution (2 min) and is subsequently exposed to a toluene solution of C_{60} ($0.2\ \text{mg/mL}$), aggregates will selectively assemble onto the hydrophobic PFT lines (Figure 4B). C_{60} aggregates assemble more readily onto the PFT regions because

of hydrophobic interactions. This also provides additional evidence for the chemical identity of the phase-separated regions. In addition to C_{60} , we have also used this procedure to selectively deposit polystyrene spheres (see Supporting Information). Interestingly, if a binary ink mixture is deposited onto a Au(111) substrate using DPN, sub-15 nm MHA structures form in the interior of dots that have diameters as large as 50 nm (Figure 4C and D).

In conclusion, binary ink mixtures of alkanethiols exhibit near-complete phase-separation behavior when deposited using micro- or nanodeposition tools, such as μ CP and DPN, a consequence of the choice of ink pairs and the different transport properties of the chosen adsorbate molecules. Interestingly, the more hydrophilic alkanethiol always forms the interior phase, while hydrophobic alkanethiols will form the outer phase when these mixtures are patterned using DPN or μ CP. This is in contrast to the bulk behavior of such adsorbates, in the context of SAMs formed from solution on gold substrates. By tailoring ink mixture composition, this phase-separation behavior can be exploited to print sub-100 nm lines in the case of μ CP and sub-15 nm lines in the case of DPN.

Acknowledgment. C.A.M. and T.B.H. acknowledge the Air Force Office of Scientific Research (AFOSR), the Defense Advanced Research Projects Agency (DARPA), the Army Research Office (ARO), and the NSF for support of this research.

Supporting Information Available: Effect of methanol atmosphere on binary ink transport in DPN, LFM images holding MHA/ODT-coated tip repeatedly on the same area, and plot of hold time versus phase size for MHA/PFT mixed ink diffusion. This material is available free of charge via the Internet at <http://pubs.acs.org>.

JA042393Y